https://ntrs.nasa.gov/search.jsp?R=19660026670 2020-03-16T20:34:28+00:00Z

United Aircraft Research Laboratories

UNITED AIRCRAFT CORPORATION

EAST HARTFORD, CONNECTICUT

Report E910461-3

Analytical Study of Catalytic Reactors for Hydrazine Decomposition

Quarterly Progress Report No. 1

April 15 - July 14, 1966

Contract No. NAS 7-458

This document contains information affecting the national defense of the United States within the meaning of the Espionage Laws, Title 18, U.S.C., Sections 793 and 794. The transmission or the revelation of its contents in any manner to an unauthorized person is prohibited by law.

REPORTED BY
A. S. Kesten

APPROVED BY
F. S. Owen
Chief, Propulsion

DATE July 1966

NO. OF PAGES 14

COPY NO. 17

Analytical Study of Catalytic Reactors for Hydrazine Decomposition

Quarterly Progress Report No. 1

April 15 - July 14, 1966

Contract No. NAS 7-458

TABLE OF CONTENTS

Report E910461-3

Analytical Study of Catalytic Reactors for Hydrazine Decomposition

Quarterly Progress Report No. 1

April 15 - July 14, 1966

Contract No. NAS 7-458

SUMMARY

The Research Laboratories of United Aircraft Corporation under Contract NAS 7-458 with the National Aeronautics and Space Administration are performing an analytical study of catalytic reactors for hydrazine decomposition. This report summarizes work performed during the first quarter from April 15, 1966 to July 14, 1966. Work during this reporting period has included preparation of the equations comprising the steady-state microscopic model of a distributed-feed catalytic reaction chamber in a form amenable to numerical solution. An iterative procedure has been developed to solve the implicit integral equations describing reactant concentration and temperature profiles in the porous catalyst particles. Numerical methods have been developed for the simultaneous solution of these equations with the equations describing the variation of reactant concentrations and temperature with axial position in the interstitial phase. A computer program utilizing these procedures is being written.

Reduction of the equations comprising the transient macroscopic model to a form amenable to numerical solution has been initiated. Overall transport coefficients have been used to define the driving forces for heat and mass transfer in terms of the temperature and concentration difference between the interstitial phase and the gas phase in the interior of the catalyst particles.

author

INTRODUCTION

Effective design of distributed-feed catalyzed monopropellant hydrazine rocket engines and gas generators requires accurate procedures for predicting the effects of the design parameters of the reactor system on the steady-state and transient performance of the system. This general capability does not now exist, although simplified methods have been developed for predicting the steady-state performance of idealized catalytic reactors (Ref. 1). These simplified methods do not adequately describe the combined processes of heat transfer, diffusion, and chemical reaction and are restricted to consideration of a single decomposition reaction at any axial location within the reaction chamber. To overcome these deficiencies, a more comprehensive theoretical analysis is required. Preliminary investigations at United Aircraft Research Laboratories have demonstrated the feasibility of such an analysis and, further, have indicated that both transient and steady-state performance characteristics can be predicted.

The objectives of this program are therefore (a) to develop computer programs for predicting the temperature and concentration distributions in monopropellant hydrazine catalytic reactors in which hydrazine can be injected at arbitrary axial locations in the reaction chamber, and (b) to perform calculations using these computer programs to demonstrate the effects of various system parameters on the performance of the reactor.

DISCUSSION

The analysis of a hydrazine engine reaction system pertains to a reaction chamber of arbitrary cross section packed with Shell 405 catalyst particles (Refs. 2, 3, 4 and 5) into which liquid hydrazine is injected at arbitrarily selected axial locations. At these locations, hydrazine injection is taken as uniform across the cross section of the chamber. Catalyst particles are represented as "equivalent" spheres with a diameter taken as a function of the particle size and shape. Both thermal and catalytic vapor phase decomposition of hydrazine and ammonia are considered in developing equations describing the concentration distributions of these reactants. Since the catalyst material is impregnated on the interior and exterior surfaces of porous particles, the diffusion of reactants into the porous structure must also be considered. In addition, the conduction of heat within the porous particles must be taken into account since the decomposition reactions are accompanied by the evolution or absorption of heat.

A treatment of the transport processes described above constitutes a general model of the reaction chamber. The analysis of the steady-state performance of a reactor based on this model can be carried out in a straight-forward manner. However, the analysis of the transient behavior of the system using this general model is quite complicated since both the reactant concentrations and the rate constants for decomposition, which are exponentially dependent on temperature, will be functions not only of time, but also of position within the catalyst particles.

To circumvent these complications, the transient behavior of the system can be analyzed by employing a second model which considers the resistance of a catalyst particle to heat and mass transfer to be concentrated in a thin film around the particle surface. In this "macroscopic" model, overall transport coefficients are used to define the driving forces for heat and mass transfer in terms of the temperature and concentration differences between the free-gas phase and the gas phase in the interior of the catalyst particles. In order to define the transport coefficients used in this model in terms of the real system parameters, the transient solutions can be obtained as functions of the transport coefficients and then extrapolated to infinite time to get the steady-state solutions in terms of these "macroscopic" parameters; these solutions can then be compared with the solutions obtained using the steady-state "microscopic" model to define the overall transport coefficients in terms of the real system parameters. Using this method, the concentrations of hydrazine and ammonia can be described as functions of time and position in the reaction chamber.

Effort during the first quarterly reporting period of Contract NAS 7-458 has involved, (a) preparation for numerical solution of the equations comprising the steady-state microscopic model of the reaction system, (b) initial programming of these equations for digital computation, and (c) initial preparation for numerical solution of the equation comprising the transient macroscopic model of the reaction system. This effort is described in detail in succeding sections of this report.

Steady-State Microscopic Model

In developing the steady-state microscopic model, the temperature and reactant concentrations in the interstitial phase (i.e., the free-fluid phase as distinguished from the gas phase within the porous particles) are assumed to vary only with axial distance along the bed. In the entrance region of the reaction chamber, where the temperature is low enough to permit the existence of liquid hydrazine, vaporization of liquid is assumed to occur as a result of decomposition of vapor hydrazine within the pores of the catalyst particles. That is, catalytic reaction is assumed to be fast enough to keep liquid hydrazine from wetting the pores of the particles; the hydrazine concentration at the surface of the catalyst particles at any axial location in the entrance region is then computed from the vapor pressure of liquid hydrazine in the interstitial phase at the same axial location. Neglecting axial diffusion of heat or mass, the change in enthalpy of the interstitial phase in the region where liquid hydrazine is present (i.e., where $h_i < h_i^V$) is related to the concentration gradient at the surface of the porous catalyst particles by

$$G \frac{dh_i}{dz} + H^{N_2H_4} D_p A_p \left(\frac{dc_p^{N_2H_4}}{dx} \right)_s + F\,(h_i - h_F) = 0 \qquad (1)$$

$$\text{for } h_i \le h_i^V$$

The variation of mass flow rate, G, with axial distance is easily computed from the rate of feed of liquid hydrazine from the distributed injectors into the system. In the region where liquid hydrazine exists at temperatures below the vaporization temperature, the temperature may be obtained from

$$T_i = T_F + \frac{h_i - h_F}{C_f} \qquad \text{for } h_i < h_i^L \qquad (2)$$

In the two-phase region, where $T_i = T_{vap}$, the weight-fraction of vapor may be computed from

$$\text{WEIGHT - FRACTION VAPOR} = \frac{h_i - h_i^L}{h_i^V - h_i^L} \qquad \text{for } h_i^L \le h_i \le h_i^V \qquad (3)$$

At the axial position at which the enthalpy of the interstitial phase is just equal to the enthalpy of vapor hydrazine at the boiling point ($h_i = h_i^V$), the fraction of hydrazine injected upstream of that point which has been decomposed is easily calculated from an overall heat balance. The associated amounts of ammonia, nitrogen, and hydrazine formed from decomposition of hydrazine can then be calculated taking the decomposition reaction as

$$2N_2H_4 \rightarrow 2NH_3 + N_2 + H_2$$

It should be noted that this is the overall reaction scheme determined experimentally for both homogeneous decompostion of hydrazine (Refs. 6, 7, 8) and low pressure heterogeneous decomposition of hydrazine on platinum surfaces (Ref. 9).

In the remainder of the reaction chamber, where $h_i > h_i^V$, heat is being supplied to the system by homogeneous as well as heterogeneous decomposition of hydrazine. In addition, at sufficiently high temperature, heat is removed from the system by the endothermic decomposition of ammonia. For $h_i > h_i^V$ then, the change in enthalpy with axial distance is related to the concentration gradients at the surface of the porous catalyst particles by

$$G\frac{dh_i}{dz} + H^{N_2H_4} r_{hom}\gamma + A_p\left[H D_p\left(\frac{dc_p}{dx}\right)_s\right]^{N_2H_4} + A_p\left[H D_p\left(\frac{dc_p}{dx}\right)_s\right]^{NH_3} + F(h_i - h_F) = 0 \tag{4}$$

The reactant concentration at the surface of the catalyst particles at any axial location is taken equal to the reactant concentration in the interstitial phase at the same axial location. The change in reactant concentrations with axial distance is related to the concentration gradients at the surface of the porous catalyst particles by

$$-\frac{R}{P}\left[c_i^{N_2H_4} T_i \frac{dG}{dz} + G T_i \frac{dc_i^{N_2H_4}}{dz} + G c_i^{N_2H_4}\frac{dT_i}{dz}\right] + F - r_{hom}\gamma - A_p\left[D_p\left(\frac{dc_p}{dx}\right)_s\right]^{N_2H_4} = 0 \tag{5}$$

$$-\frac{R}{P}\left[c_i^{NH_3} T_i \frac{dG}{dz} + G T_i \frac{dc_i^{NH_3}}{dz} + G c_i^{NH_3}\frac{dT_i}{dz}\right] + r_{hom}\gamma\frac{M^{NH_3}}{M^{N_2H_4}} + A_p\left[D_p\left(\frac{dc_p}{dx}\right)_s\right]^{N_2H_4}\frac{M^{NH_3}}{M^{N_2H_4}} - A_p\left[D_p\left(\frac{dc_p}{dx}\right)_s\right]^{NH_3} = 0 \tag{6}$$

$$- \frac{R}{P} \left[c_i^{N_2} T_i \frac{dG}{dz} + G T_i \frac{dc_i^{N_2}}{dz} + G c_i^{N_2} \frac{dT_i}{dz} \right] + \frac{1}{2} r_{hom} \gamma \frac{M^{N_2}}{M^{N_2H_4}}$$

$$+ \frac{A_p}{2} \left[D_p \left(\frac{dc_p}{dx} \right)_s \right]^{N_2H_4} \frac{M^{N_2}}{M^{N_2H_4}} + \frac{A_p}{2} \left[D_p \left(\frac{dc_p}{dx} \right)_s \right]^{NH_3} \frac{M^{N_2}}{M^{NH_3}} = 0 \tag{7}$$

$$- \frac{R}{P} \left[c_i^{H_2} T_i \frac{dG}{dz} + G T_i \frac{dc_i^{H_2}}{dz} + G c_i^{H_2} \frac{dT_i}{dz} \right] + \frac{1}{2} r_{hom} \gamma \frac{M^{H_2}}{M^{N_2H_4}}$$

$$+ \frac{A_p}{2} \left[D_p \left(\frac{dc_p}{dx} \right)_s \right]^{N_2H_4} \frac{M^{H_2}}{M^{N_2H_4}} + \frac{3A_p}{2} \left[D_p \left(\frac{dc_p}{dx} \right)_s \right]^{NH_3} \frac{M^{H_2}}{M^{NH_3}} = 0 \tag{8}$$

The temperature of the interstitial phase in this region is related to the enthalpy by

$$h_i - h_i^V = \int_{T_{vap}}^{T_i} C_f \, dT_i \tag{9}$$

where C_f is the specific heat of the gas mixture and is a function of temperature as well as the concentration of the constituents of the mixture.

The reactant concentration profile in the porous particles at any axial location must satisfy the diffusion equation for mass transport as well as an analogous equation for heat conduction. Neglecting the effect of the translational motion of the gas stream on diffusion within the porous particles and assuming constant diffusion coefficients, D_p, and thermal conductivities, K_p, these equations may be written as

$$D_p \nabla^2 c_p - r_{het} = 0 \tag{10}$$

$$K_p \nabla^2 T_p - H r_{het} = 0 \tag{11}$$

Using Eqs. (10) and (11), Prater (Ref. 10) has pointed out that temperature and concentration are related quite simply by

$$T_p - (T_p)_s = -\frac{HD_p}{K_p}\left[(c_p)_s - c_p\right] \tag{12}$$

The use of this relationship enables the reaction rate, r_{het}, to be written as a function of concentration alone instead of concentration and temperature. Equation (10) can then be solved for the concentration at any point in the porous particle in terms of the concentration at the surface of the particle, $(c_p)_s = c_i$. The solution is derived in Appendix A as an implicit integral equation given by

$$c_p(x) = c_i - \left[\frac{1}{x} - \frac{1}{a}\right]\int_0^x \xi^2 \frac{r_{het}(c_p)}{D_p}\, d\xi - \int_x^a \left[\frac{1}{\xi} - \frac{1}{a}\right] \xi^2 \frac{r_{het}(c_p)}{D_p}\, d\xi \tag{13}$$

Simultaneous solution of Eq. (13) with the appropriate equations describing the changes in enthalpy and reactant concentrations in the interstitial phase with axial distance will yield the steady-state temperature and concentration profiles in the reaction chamber.

Finite difference methods are being used to program for digital computation the ordinary differential equations describing the changes in enthalpy and reactant concentrations in the interstitial phase. No iteration is necessary to solve these equations numerically. However, Eq. (13), which must be solved simultaneously with the differential equations, is an implicit integral equation which requires an iterative procedure for solution. Hand calculations, using Arrhenius type expressions for the rate of reaction, r_{het}, have indicated that convergence to a solution for $c_p(x)$ is difficult to achieve unless the initial estimate of the concentration distribution is fairly accurate. Methods have been developed for generating this estimate and an iterative procedure has been devised which effects rapid convergence over a fairly wide range of anticipated conditions. This procedure has been programmed for digital computation and is presently being debugged. The procedure will then be used as a subroutine in the main program representing the steady-state microscopic model.

Transient Macroscopic Model

In developing the transient macroscopic model, the concentrations of reactants in the interstitial phase are assumed to vary only with time and axial distance along the bed. In this system, the rate of mass transfer between the interstitial phase and the gas phase within the porous particles is expressed in terms of an overall mass transfer coefficient, k_s, as $k_s A_p (c_i - c_p)$. Similarly an overall heat transfer coefficient, h_s, is used to describe the rate of heat transfer as

$h_s A_p (T_i - T_p)$. The concentration, c_p, and the temperature, T_p, are taken as uniform within the interior of the porous particles. These assumptions lead to a series of first-order, partial differential equations for the temperature and reactant concentrations in the interstitial phase which must be solved simultaneously with first-order, ordinary differential equations for the temperature and reactant concentrations in the gas phase within the porous particles. These equations are currently being formulated into a network of first-order, ordinary differential equations which can be solved numerically using a reasonably simple computational scheme.

REFERENCES

1. Grant, A. F., Jr.: Basic Factors Involved in the Design and Operation of Catalytic Monopropellant-Hydrazine Reaction Chambers. Jet Propulsion Laboratory Report No. 20-77, December 31, 1954.

2. Armstrong, W. E., D. S. LaFrance, and H. H. Voge: Development of Catalysts for Monopropellant Decomposition of Hydrazine (U). Part I, Experimental Studies (Confidential). Part II, Engineering Calculations (Confidential). Shell Development Company Report S-13864, 1962.

3. Armstrong, W. E., R. D. Hawthorn, D. S. LaFrance, C. Z. Morgan, L. B. Ryland, and H. H. Voge: Development of Catalysts for Monopropellant Decomposition of Hydrazine (U). Shell Development Company Report S-13889, 1963. (Confidential)

4. Armstrong, W. E., C. Z. Morgan, L. B. Ryland, and H. H. Voge: Development of Catalysts for Monopropellant Decomposition of Hydrazine (U). Shell Development Company Report S-13917, 1964. (Confidential)

5. Armstrong, W. E., C. Z. Morgan, L. B. Ryland, and H. H. Voge: Development of Catalysts for Monopropellant Decomposition of Hydrazine (U). Shell Development Company Report S-13947, 1964. (Confidential)

6. Eberstein, I. J., and I. Glassman: The Gas-Phase Decomposition of Hydrazine and Its Methyl Derivations. Tenth Symposium (International) on Combustion, Pittsburgh, The Combustion Institute, 1965, pp. 365-374.

7. McHale, E. T., B. E. Knox, and H. B. Palmer: Determination of the Decomposition Kinetics of Hydrazine Using a Single-Pulse Shock Tube. Tenth Symposium (International) on Combustion, The Combustion Institute, Pittsburgh, 1965, pp. 341-351.

8. Michel, K. W., and H. GG. Wagner: The Pyrolysis and Oxidation of Hydrazine Behind Shock Waves. Tenth Symposium (International) on Combustion, The Combustion Institute, Pittsburgh, 1965, pp. 353-364.

9. Askey, P. J.: The Thermal Decomposition of Hydrazine. J. Am. Chem. Soc., Vol. 52, 1930, pp. 970-974.

10. Prater, D. C.: The Temperature Produced by Heat of Reaction in the Interior of Porous Particles. Chemical Engineering Science, Vol. 8, 1958, pp. 284-286.

11. Irving, J., and N. Mullineux: Mathematics in Physics and Engineering. Academic Press, Inc., New York, 1959, p. 731.

LIST OF SYMBOLS

a	Radius of spherical particle
A_p	Total external surface area of catalyst particle per unit volume of bed
c_i	Reactant concentration in interstitial fluid
c_p	Reactant concentration in gas phase within the porous particle
c_p^*	Equals $c_p - c_i$
C_f	Specific heat of fluid in the interstitial phase
D_p	Diffusion coefficient of reactant gas in the porous particle
F	Rate of feed of reactant into the system
G	Mass flow rate or Green's function (defined in Appendix I)
h	Enthalpy
$\mathscr{h}_s$	Overall heat transfer coefficient
H	Heat of reaction (negative for exothermic reaction)
K_p	Thermal conductivity of reactant gas in the porous particle
k_s	Overall mass transfer coefficient
M	Molecular weight
P	Chamber pressure
r_{het}	Rate of (heterogeneous) chemical reaction on the catalyst surfaces
r_{hom}	Rate of (homogeneous) chemical reaction in the interstitial phase
R	Gas constant
T	Temperature
u	Mathematical function (defined in Appendix I)

LIST OF SYMBOLS (cont'd)

v	Mathematical function (defined in Appendix I)
x	Radial distance from the center of the spherical particle
z	Axial distance
γ	Fractional void volume of bed
ϕ	Mathematical function (defined in Appendix I)

Subscripts

F	Refers to feed
i	Refers to interstitial phase
p	Refers to gas within the porous particle
s	Refers to particle surface

Superscripts

L	Refers to liquid at vaporization temperature
V	Refers to vapor at vaporization temperature

APPENDIX I

DERIVATION OF INTEGRAL EQUATIONS REPRESENTING THE CONCENTRATION PROFILES OF REACTANTS WITHIN THE CATALYST PARTICLES

In this section equations are developed to describe the steady-state concentration profiles of hydrazine vapor and of ammonia within the catalyst particles. The reactant concentration profiles in the porous particles at any axial location can be found as solutions to:

$$D_p \nabla^2 c_p - r_{het}(c_p) = 0 \tag{I-1}$$

If the catalyst particles are taken to be "equivalent" spheres of radii a, and if concentration c_p^* is defined such that $c_p^* = c_p - c_i$, Eq. (I-1) can be written as

$$D_p \left[\frac{1}{x^2} \frac{d}{dx} \left(x^2 \frac{dc_p^*}{dx} \right) \right] - r_{het} = 0 \tag{I-2}$$

where x is the radial distance from the center of a sphere. The boundary conditions associated with Eq. (I-2) are

$$c_p^* = 0 \quad \text{AT} \quad x = a, \qquad \frac{dc_p^*}{dx} = 0 \quad \text{AT} \quad x = 0 \tag{I-3}$$

Equation (I-2) can be rearranged to get

$$\frac{d}{dx}\left(x^2 \frac{dc_p^*}{dx} \right) = \frac{r_{het}\, x^2}{D_p} = \phi(x, c_p^*) \tag{I-4}$$

The solution to Eq. (I-4) is most easily obtained by converting it into a Fredholm integral equation (see Ref. 11) of the form

$$c_p^*(x) = \frac{1}{x^2 \left[u(x)\, v'(x) - u'(x)\, v(x) \right]} \int_0^a G(x, \xi)\, \phi(\xi, c_p^*)\, d\xi \tag{I-5}$$

where $u(x)$ is a solution of

$$\frac{d}{dx}\left(x^2 \frac{du}{dx}\right) = 0 \qquad \text{(I-6)}$$

subject to the condition that

$$\left[u \frac{dc_p^*}{dx} - \frac{du}{dx} c_p^*\right]_{x=0} = 0 \qquad \text{(I-7)}$$

and $v(x)$ is a solution of

$$\frac{d}{dx}\left(x^2 \frac{dv}{dx}\right) = 0 \qquad \text{(I-8)}$$

subject to the condition that

$$\left[v \frac{dc_p^*}{dx} - \frac{dv}{dx} c_p^*\right]_{x=a} = 0 \qquad \text{(I-9)}$$

The Green's function, $G(x,\xi)$ is given by

$$G(x,\xi) = \begin{cases} u(\xi)\, v(x) & \text{FOR} \quad 0 \leq \xi \leq x \\ u(x)\, v(\xi) & \text{FOR} \quad x \leq \xi \leq a \end{cases} \qquad \text{(I-10)}$$

The function $u(x)$ can be determined by first integrating Eq. (I-6) to get

$$u = -\frac{A_1}{x} + B_1 \qquad \text{(I-11)}$$

Applying Eq. (I-7) together with the first of boundary conditions (I-3) to Eq. (I-11), it is found that $A = 0$ and

$$u = B_1 \qquad \text{(I-12)}$$

The function $v(x)$ can be determined in a similar manner by first integrating Eq. (I-8) to get

$$v = -\frac{A_2}{x} + B_2 \qquad \text{(I-13)}$$

and then applying Eq. (I-9) and the second of boundary conditions (I-3) to Eq. (I-13) to get

$$v = A_2\left[\frac{1}{a} - \frac{1}{x}\right] \qquad \text{(I-14)}$$

Equations (I-10), (I-12), and (I-14) can now be combined to get

$$G(x,\xi) = \begin{cases} A_2B_1\left[\frac{1}{a} - \frac{1}{x}\right] & \text{FOR} \quad 0 \le \xi \le x \\ A_2B_1\left[\frac{1}{a} - \frac{1}{\xi}\right] & \text{FOR} \quad x \le \xi \le a \end{cases} \qquad \text{(I-15)}$$

In addition,

$$x^2\left[u(x)\,v'(x) - u'(x)\,v(x)\right] = A_2B_1 \qquad \text{(I-16)}$$

Equations (I-15) and (I-16) can now be substituted into Eq. (I-5) to get

$$c_p^*(x) = \left[\frac{1}{a} - \frac{1}{x}\right]\int_0^x \phi(\xi, c_p^*)\,d\xi + \int_x^a \left[\frac{1}{a} - \frac{1}{\xi}\right]\phi(\xi, c_p^*)\,d\xi \qquad \text{(I-17)}$$

or

$$c_p(x) = c_i - \left[\frac{1}{x} - \frac{1}{a}\right]\int_0^x \xi^2\,\frac{r_{het}(c_p)}{D_p}\,d\xi - \int_x^a \left[\frac{1}{\xi} - \frac{1}{a}\right]\xi^2\,\frac{r_{het}(c_p)}{D_p}\,d\xi \qquad \text{(I-18)}$$

Equation (I-18) is an implicit integral equation which can be solved numerically to determine the concentration at any point in a porous particle in terms of c_i, the concentration at the surface of the particle. The gradients of c_p, evaluated at the particle surfaces at given axial locations, can then be obtained from the slopes of curves of c_p versus x at $x=a$.

ESTIMATED PROGRESS SCHEDULE

CUMULATIVE TOTAL EXPENDITURES *

NAS 7 - 458

*EXCLUSIVE OF FEE

TOTAL EXPENDITURES (DOLLARS): 56,738

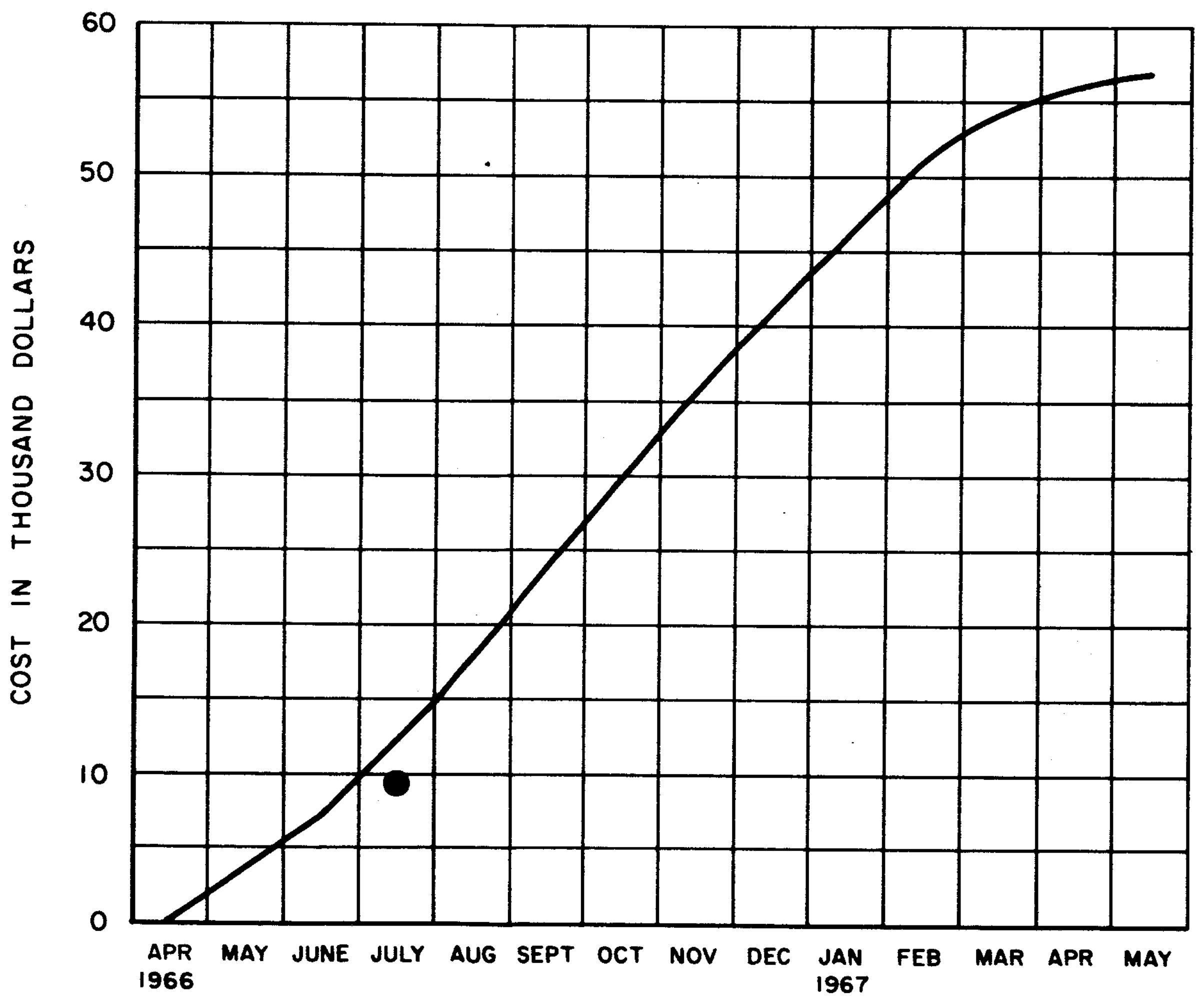

ESTIMATED PROGRESS SCHEDULE

CUMULATIVE DIRECT LABOR

NAS 7 - 458

TOTAL MAN-HOURS: 4790

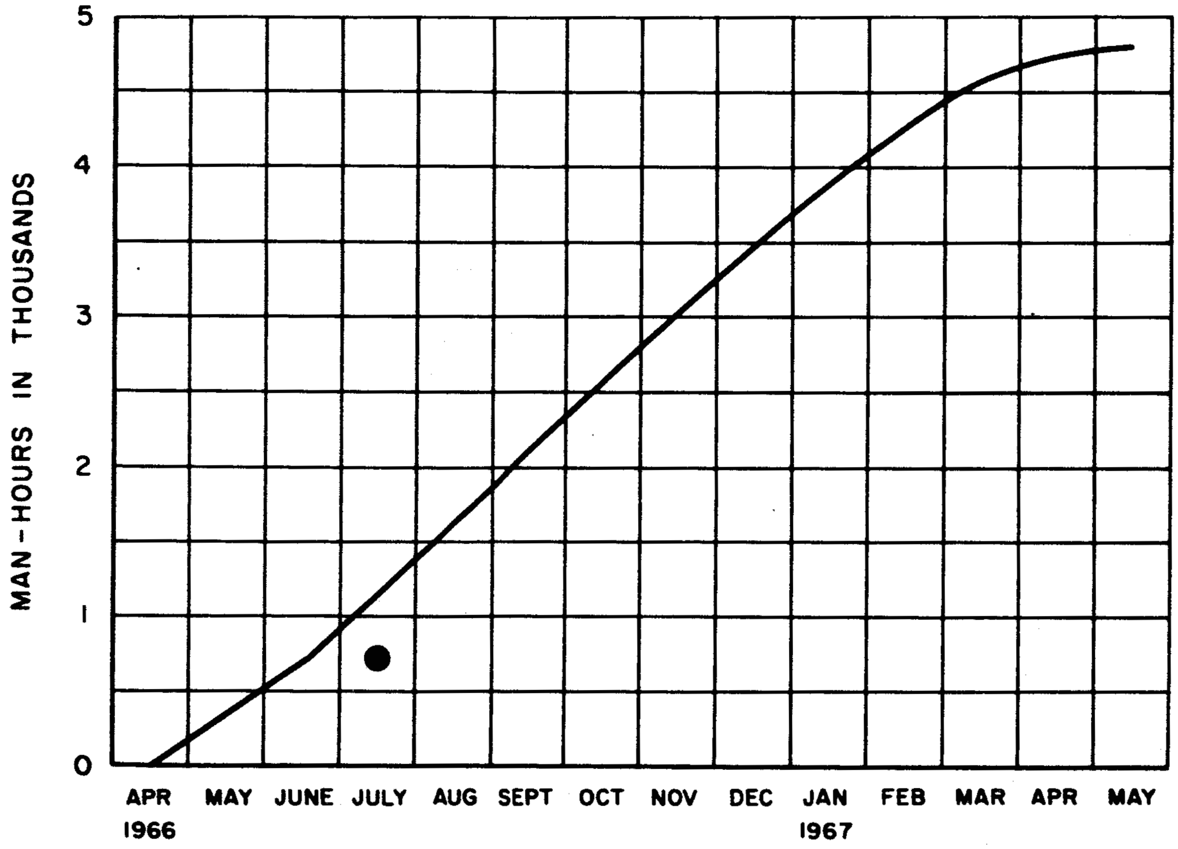

DISTRIBUTION LIST FOR MONTHLY/QUARTERLY REPORTS
(Contract NAS 7-458)

Addressee	No. of Copies
National Aeronautics and Space Administration NASA Resident Office Jet Propulsion Laboratory 4800 Oak Grove Drive Pasadena, California 91103A Attn: Mr. James S. Evans Contracting Officer, T-93	3
Jet Propulsion Laboratory 4800 Oak Grove Drive Pasadena, California 91103 Attn: Mr. T. W. Price	1
AFRPL (RPRED) Edwards Air Force Base, California 93523 Attn: Mr. K. O. Rimer	1
U. S. Naval Ordnance Test Station China Lake, California 93557 Attn: Mr. J. O. Dake, Code 4505	1
NASA Headquarters Washington, D. C. 20546 Attn: Mr. R. H. Rollins, II, Code RPX	1
NASA Headquarters Washington, D. C. 20546 Attn: Dr. R. Levine, Code RPL	1
NASA Headquarters Washington, D. C. 20546 Attn: Mr. C. H. King, Code MAT	1
National Aeronautics and Space Administration Manned Spacecraft Center Houston, Texas 77058 Attn: Mr. H. A. Pohl	1
National Aeronautics and Space Administration Lewis Research Center 21000 Brookpark Road Cleveland, Ohio 44135 Attn: Mr. I. A. Johnsen	1

DISTRIBUTION LIST FOR MONTHLY/QUARTERLY REPORTS
(Contract NAS 7-458)

Addressee	No. of Copies
National Aeronautics and Space Administration Langley Research Center Langley Station Hampton, Virginia 23365 Attn: Mr. Robert L. Swain	1
Jet Propulsion Laboratory 4800 Oak Grove Drive Pasadena, California 91103 Attn: Mr. D. D. Evans	1
National Aeronautics and Space Administration Goddard Space Flight Center Greenbelt, Maryland 20771 Attn: Mr. D. J. Grant	1
National Aeronautics and Space Administration George C. Marshall Space Flight Center Redstone Arsenal Huntsville, Alabama 35812 Attn: Mr. J. Thompson	1
Air Force Office of Scientific Research Washington, D. C. 20546 Attn: Lt. Col. John Donovan	1
Scientific and Technical Information Facility P. O. Box 5700 Bethesda, Maryland 20014 Attn: NASA Representative, Code CRT	1